Global Change Biology WILEY

RESEARCH ARTICLE

Damage to living trees contributes to almost half of the biomass losses in tropical forests

Daniel Zuleta[1] | Gabriel Arellano[2,3] | Sean M. McMahon[1,4] | Salomón Aguilar[5] | Sarayudh Bunyavejchewin[6] | Nicolas Castaño[7] | Chia-Hao Chang-Yang[8] | Alvaro Duque[9] | David Mitre[5] | Musalmah Nasardin[10] | Rolando Pérez[5] | I-Fang Sun[11] | Tze Leong Yao[10] | Renato Valencia[12] | Sruthi M. Krishna Moorthy[13,14] | Hans Verbeeck[14] | Stuart J. Davies[1]

[1]Forest Global Earth Observatory, Smithsonian Tropical Research Institute, Washington, District of Columbia, USA

[2]Ecology and Evolutionary Biology, University of Michigan, Ann Arbor, Michigan, USA

[3]Oikobit LLC, Albuquerque, New Mexico, USA

[4]Smithsonian Environmental Research Center, Edgewater, Maryland 21037, USA

[5]Smithsonian Tropical Research Institute, Apartado 0843-03092, Balboa, República de Panamá

[6]Department of National Parks, Forest Research Office, Wildlife and Plant Conservation, Bangkok, 10900, Thailand

[7]Herbario Amazónico Colombiano, Instituto Amazónico de Investigaciones Científicas Sinchi, Bogotá, Colombia

[8]Department of Biological Sciences, National Sun Yat-sen University, Kaohsiung, 80424, Taiwan

[9]Departamento de Ciencias Forestales, Universidad Nacional de Colombia Sede Medellín, Medellín, Colombia

[10]Forestry and Environment Division, Forest Research Institute Malaysia, 52109, Kepong, Selangor, Malaysia

[11]Center for Interdisciplinary Research on Ecology and Sustainability, National Dong Hwa University, Hualien, 94701, Taiwan

[12]Escuela de Ciencias Biológicas, Pontificia Universidad Católica del Ecuador, Quito, Ecuador

[13]Department of Geographical Sciences, University of Maryland, College Park, Maryland, USA

[14]Department of Environment, Ghent University, Ghent, Belgium

Correspondence
Daniel Zuleta, Forest Global Earth Observatory, Smithsonian Tropical Research Institute, 10th St. and Constitution Ave. NW, Washington, DC 20560, USA.
Email: dfzuleta@gmail.com

Abstract

Accurate estimates of forest biomass stocks and fluxes are needed to quantify global carbon budgets and assess the response of forests to climate change. However, most forest inventories consider tree mortality as the only aboveground biomass (AGB) loss without accounting for losses via damage to living trees: branchfall, trunk breakage, and wood decay. Here, we use ~151,000 annual records of tree survival and structural completeness to compare AGB loss via damage to living trees to total AGB loss (mortality + damage) in seven tropical forests widely distributed across environmental conditions. We find that 42% ($3.62\,\mathrm{Mg\,ha^{-1}\,year^{-1}}$; 95% confidence interval [CI] 2.36–5.25) of total AGB loss ($8.72\,\mathrm{Mg\,ha^{-1}\,year^{-1}}$; CI 5.57–12.86) is due to damage to living trees. Total AGB loss was highly variable among forests, but these differences were mainly caused by site variability in damage-related AGB losses rather than by mortality-related AGB losses. We show that conventional forest inventories overestimate stand-level AGB stocks by 4% (1%–17% range across forests) because assume structurally complete trees, underestimate total AGB loss by 29% (6%–57% range across forests) due to overlooked damage-related AGB losses, and overestimate AGB

loss via mortality by 22% (7%–80% range across forests) because of the assumption that trees are undamaged before dying. Our results indicate that forest carbon fluxes are higher than previously thought. Damage on living trees is an underappreciated component of the forest carbon cycle that is likely to become even more important as the frequency and severity of forest disturbances increase.

1 | INTRODUCTION

Large spatial and temporal uncertainty governs forest carbon stocks and fluxes, especially in the tropics (Duque et al., 2021; Harris et al., 2021; Requena Suarez et al., 2019; Xu et al., 2021). Resolving key components of biomass estimates is critical for quantifying the global carbon budget, informing forest-based solutions to climate change, and improving predictions on the fate of these ecosystems and climate-vegetation feedbacks (Cabon et al., 2022; Friedlingstein et al., 2022; Kolby Smith et al., 2016; Muller-Landau et al., 2021).

Forest carbon fluxes are typically estimated from repeated ground-based inventories of individual trees (Clark, Brown, Kicklighter, Chambers, Thomlinson, & Ni, 2001). Tree-level biomass is obtained from allometric models that relate living, aboveground biomass (AGB) of structurally healthy [i.e., undamaged (Clark & Kellner, 2012)] trees with variables collected in the field, primarily tree diameter and species' wood density. Over time, repeated measurements of these tree-level variables on surviving trees plus the AGB of newly recruited trees are used to estimate AGB gains via tree growth and recruitment. The AGB of dead trees is used as an estimate of AGB loss (Chave et al., 2003; Hubau et al., 2020; Piponiot et al., 2022). Under this approach, the allometry-based AGB of a given tree remains in the system as long as it is reported alive, without looking up to assess whether the tree has experienced AGB loss via breakage or other forms of biomass losses, including branch shedding and wood decay (hereafter damage). Ignoring how much biomass remains in damaged but living trees (hereafter tree structural completeness) results in (i) an overestimation of AGB stocks because not all living trees are undamaged, (ii) an underestimation of total AGB loss by excluding damage from living trees, and (iii) an overestimation of AGB loss via tree mortality because trees are assumed to be undamaged before dying. Assessing tree structural completeness in the field is challenging, and so the AGB losses due to damage to living trees are rarely quantified in ground-based estimates of forest carbon fluxes (Chambers et al., 2001; Chave et al., 2003; Clark & Kellner, 2012).

Small-scale forest disturbances such as branchfall are much more frequent than large-scale disturbances (Espírito-Santo et al., 2014; Solé & Manrubia, 1995). Woody debris surveys (Anderson-Teixeira et al., 2021; Chao et al., 2022; Clark, Brown, Kicklighter, Chambers, Thomlinson, & Holland, 2001; Gora et al., 2019; Maass et al., 2002;

Malhi et al., 2014; Palace et al., 2008), drone-derived canopy disturbance estimates (Araujo et al., 2021; Cushman et al., 2022), airborne LiDAR data (Dalagnol et al., 2021; Leitold et al., 2022; Marvin & Asner, 2016), and more detailed ground-based forest inventories (Chambers et al., 2001; Chave et al., 2003) suggest that branchfall can contribute to 15%–47% of total AGB losses in tropical forests. However, these approaches are not able to distinguish whether this AGB loss comes from dead trees already counted as AGB loss in forest inventories or from damaged but surviving trees assumed to be structurally healthy if their diameter is reported. While damage to living trees is expected to be a major contributor to total AGB loss, its importance relative to mortality-based AGB loss is yet to be quantified.

Accounting for AGB losses from damaged but living trees may not be that important if damaged trees die in the short term. Indeed, tree damage has been identified as one of the most common conditions preceding tree death (Arellano et al., 2019; Reis et al., 2022; Zuleta, Arellano, et al., 2022). Damaged trees may be more likely to die because of the loss of photosynthetic capacity that leads to carbon starvation (McDowell et al., 2008), large energetic costs of repair (Anderegg et al., 2012), higher structural vulnerability to windthrows (Csilléry et al., 2017), and exposure of live tissues to pathogen infections and pests (Dyer et al., 2012; McDowell et al., 2022). If damage and mortality are strongly coupled, AGB losses from tree mortality would just be the time-integrated estimate of AGB loss for each tree. However, not all damaged trees die in the short term. Zuleta, Arellano, et al. (2022), showed that tree damage contributed to 22%–45% of mortality across six tropical forests because of a combination of high prevalence (i.e., many trees got damaged) and moderate lethality. As a result, large proportions of damaged trees survived every year and recovered. Resolving the timing of these damage and mortality interactions will provide a comprehensive assessment of the role of non-lethal biomass losses from living trees in estimates of forest biomass fluxes.

Here, we use annual records on the survival and structural completeness of 36,511 trees (2467 species) collected across 29 censuses in seven tropical forests to estimate and compare AGB losses via tree mortality (hereafter mortality-related AGB losses) with AGB losses via damage to living trees (hereafter damage-related AGB losses). We estimate how these AGB losses vary within and among sites, assess damage–mortality interactions,

and compare estimates of AGB stocks and fluxes accounting for tree completeness (i.e., considering damage) against conventional approaches based only on tree diameter and mortality (i.e., without considering damage).

2 | MATERIALS AND METHODS

2.1 | Study sites

This study was carried out in seven 24–50 ha tropical forest dynamics plots of the ForestGEO network (Davies et al., 2021) distributed across the Neotropics (Amacayacu, Colombia; Barro Colorado Island [BCI], Panamá; Yasuní, Ecuador) and Asia (Fushan, Taiwan; Huai Kha Khaeng [HKK], Thailand; Khao Chong [KC], Thailand; Pasoh, Malaysia). At each plot, all trees with a diameter at the point of measurement (dbh) ≥ 1 cm were mapped, measured, and collected for taxonomic identification. The sites span a wide range of climate (from ever-wet to seasonally dry forests) and natural disturbance regimes (cyclones, local landslides, fire, droughts), as well as contrasting edaphic and topographic conditions within plots (Table S1).

2.2 | Sampling design

We studied 39,524 stems of 36,511 individual trees in 2467 species (2895 species × site combinations) (Table S1). In each site, we examined cohorts of 4464–8447 stems (average 5646) with dbh ≥ 1 cm that were alive in the most recent full census of the plot. These trees were selected based on a nested sampling designed to capture the diversity of species, tree size ranges, topography, and main environmental features within plots. Details of the sampling design, the field methods, and their rationale are provided by Arellano et al. (2021).

2.3 | Tree survival and structural completeness

We evaluated the survival status and structural completeness of the sampled trees following the ForestGEO Tree Mortality and Damage protocol (Arellano et al., 2021). Depending on the site, each tree was visited annually from two to six times between 2016 and 2022, making a total of 151,208 trees × census observations in 22 census intervals (hereafter periods) (Zuleta et al., 2023) (Table S1). The first census was used to establish the initial aboveground structural completeness of the trees and subsequent censuses were used to assess tree survival (dead/alive) and the structural completeness of surviving trees.

For each tree in each census, we calculated AGB following conventional allometries and incorporated damage as a reduction in trunk volume and crown volume to estimate the AGB of damaged trees. The AGB and total tree height of each tree were first estimated from allometries based on the species' wood density, the stem dbh, and a site-specific environmental stress variable (hereafter $AGB_{without-considering-damage}$ and $H_{without-considering-damage}$, respectively) (equations 7 and 6a, respectively, in Chave et al., 2014; Réjou-Méchain et al., 2017). For stems measured at a height >1.3 m, we obtained the corrected dbh at 1.30 m by applying a taper equation following Cushman et al. (2021). Strangler figs with unreliable measurements of size (dbh > 50 cm) were excluded from the analysis. Since Fushan is a typhoon-prone forest in which trees have a lower tree height compared to other pantropical sites, we used a local allometry to estimate $H_{without-considering-damage}$ (McEwan et al., 2011) and combined it with equation (4) in Chave et al. (2014) to estimate $AGB_{without-considering-damage}$ in this site. We truncated $H_{without-considering-damage}$ to the maximum tree height reported in each site (Table S1). We obtained the wood density of each tree based on its taxonomic identity using the BIOMASS R package (Réjou-Méchain et al., 2017; Zanne et al., 2009). When species-level values were not available, we used genus-level, family-level, or the site average. For multi-stemmed trees, tree-level $AGB_{without-considering-damage}$ was calculated as the sum of $AGB_{without-considering-damage}$ of all living stems.

We then re-scaled the $AGB_{without-considering-damage}$ by the tree volume completeness to estimate the remaining AGB in damaged trees ($AGB_{considering-damage}$). Tree volume completeness was estimated by coupling field-based damage estimates (Arellano et al., 2021) and vertical volume profile models obtained from 177 trees (49 species) scanned with high-resolution 3D terrestrial laser (TLS) in BCI (Zuleta, Krishna Moorthy, et al., 2022). The damage-related variables estimated in the field were (1) the living length of the main axis ($H_{considering-damage}$), in meters, which provides an estimate of the amount of remaining living tissues along the main axis of the stem (e.g., the height of breakage or the height discounting wood decay) and (2) the remaining proportion of branch volume within the living length ($b \in [0, 1]$). Both $H_{considering-damage}$ and b were only recorded in the field when there was evidence of recent damage at the time of assessment (Arellano et al., 2021).

To translate from the field-based damage variables to AGB estimates, we used a model that describes the cumulative relative volume of the trunk and crown at a relative height within a given tree ($h \in [0, 1]$) (Ver Planck & MacFarlane, 2014; Zuleta, Krishna Moorthy, et al., 2022) (Equations 1 and 2). If h is below the relative height of the lowest branch, $h_{lowest-branch} \in [0, 1]$, the total accumulated relative volume of the tree equals the accumulated relative volume of the trunk, $v_{trunk}(h) \in [0, 1]$. If h is equal to or higher than $h_{lowest-branch}$, the total accumulated relative volume of the tree is the sum of $v_{trunk}(h)$ and the accumulated relative volume of the crown, $v_{crown}(h) \in [0, 1]$:

$$v_{trunk}(h) = p_{trunk} \times \left(1 - (1-h)^{\alpha_1}\right) \tag{1}$$

$$v_{crown}(h) = \left(\frac{1 - v_{trunk}(h = h_{lowest-branch})}{1 - h_{lowest-branch}^{\alpha_2}}\right) \times \left(1 - \left(1 - (h - h_{lowest-branch})\right)^{\alpha_2}\right) \tag{2}$$

where p_{trunk} is the estimated proportion of volume in the trunk of tropical trees, and α_1 and α_2 are tapering parameters that describe the rate

of woody volume accumulation in the trunk and crown, respectively. We set $p_{trunk} = 0.73$, $\alpha_1 = 2.622$, $\alpha_2 = 6.957$, and $h_{lowest-branch} = 0.42$ based on data from the trees scanned with the terrestrial laser (Zuleta, Krishna Moorthy, et al., 2022).

The remaining AGB in a damaged tree $(AGB_{considering-damage})$ was finally estimated as the AGB of the tree assuming no damage $(AGB_{without-considering-damage})$ multiplied by the sum of the remaining relative volume in the trunk $\left(v_{trunk}\left[h = (H_{considering-damage}) / (H_{without-considering-damage})\right]\right)$ plus the remaining relative volume in the crown $\left(b \times v_{crown}\left[h = (H_{considering-damage}) / (H_{without-considering-damage})\right]\right)$ (Equation 3):

$$AGB_{considering-damage} = AGB_{without-considering-damage}$$
$$\times \left(v_{trunk}\left(h = \frac{H_{considering-damage}}{H_{without-considering-damage}}\right) + b \times v_{crown}\left(h = \frac{H_{considering-damage}}{H_{without-considering-damage}}\right)\right)$$
$$(3)$$

2.4 | AGB stocks and losses

For each period and site, the mortality-related AGB loss was estimated based on the $AGB_{considering-damage}$ of alive trees at the beginning of the period that were found dead at the end of the period. The damage-related AGB loss was estimated as the difference in $AGB_{considering-damage}$ at the beginning and at the end of each period for the trees that got damaged (i.e., lost sections of their trunks/branches) but survived. Total AGB loss was estimated as the sum of mortality-related AGB loss and damage-related AGB loss for each site and period. From year to year, some trees may seem to increase their estimated $AGB_{considering-damage}$ due to unmeasured tree growth and/or measurement error. We allowed tree-level increases in $AGB_{considering-damage}$ up to +20% per year and adjusted the $AGB_{considering-damage}$ time series of each tree to minimize unreliable losses. We performed sensitivity analysis and found that our results were robust to this methodological choice (Figure S1). To provide comparisons with the conventional approach (i.e., estimating AGB losses only from tree mortality assuming undamaged trees), we also estimated AGB stocks and losses based only on $AGB_{without-considering-damage}$. To infer patterns at the full 24–50 ha plot scale from our stratified sample, tree individuals were weighted by the frequency of their [size class × species] bins within the forest plot relative to their frequency in the sample following Zuleta, Arellano, et al. (2022).

Forest-wide AGB loss rates ($Mg\,ha^{-1}\,year^{-1}$) were finally estimated in each plot following equation (6) in Kohyama et al. (2019): AGB loss rate $\left(Mg\,ha^{-1}year^{-1}\right) = (AGB_0 - AGB_{S0}) / T$, where AGB_0 and AGB_{S0} are the estimated weighted AGB at the beginning of the period and the estimated weighted AGB of survivors at the end of each period within fixed tree cohorts, respectively; T is the average annualized time census interval. To make fair comparisons across forests, AGB loss rates were also estimated as the percentage of initial biomass [i.e., specific rate of biomass loss; equation (9) in Kohyama et al., 2019] in each period as: AGB relative loss rate $\left(\%\,year^{-1}\right) = \left(\log(AGB_0 / AGB_{S0}) / T\right) \times 100$.

2.5 | Uncertainty and confidence intervals

There are many sources of error and uncertainty in AGB estimates (i.e., field observations and measurements, allometric models, parameter estimation, etc.) (Muller-Landau et al., 2021). We compared our $AGB_{considering-damage}$ estimates with TLS-derived AGB (AGB_{TLS}) calculations from 159 trees in BCI to have an estimate of the overall error in our AGB metrics. TLS data were collected from 25 subplots of $40\,m \times 40\,m$ (total $60\,m \times 60\,m$ to account for edge effects) within the 50-ha plot on BCI between January and March 2019 using a commercial scanner (RIEGL VZ-400 with a narrow infrared laser beam of wavelength 1550 nm and a beam divergence of 0.35 mrad) (Krishna Moorthy et al., 2022). In each subplot, TLS data were collected from locations spaced 15 m apart (25 scans per subplot). We registered the point clouds from these 25 locations into a single high-resolution point cloud per subplot using the RISCAN Pro software (version 2.5.3; RIEGL Laser Measurement Systems GmbH). We manually segmented the individual trees from the plot-level point clouds using the open-source CloudCompare software (version 2.10.2) (CloudCompare, 2021). The total wood volume of each tree was estimated by fitting Quantitative Structure Models (QSMs) using the TreeQSM algorithm (Krishna Moorthy et al., 2020; Raumonen et al., 2013). Overall, $AGB_{considering-damage}$ and AGB_{TLS} were highly correlated (Pearson' product–moment correlation = 0.90, $p < .001$; Figure S2a). Assuming AGB_{TLS} as the observed AGB value of any given tree, the average relative error of our $AGB_{considering-damage}$ estimates (estimated minus observed AGB, divided by observed AGB, in %) was 10.2% across the 159 trees (SE = 3.01, Figure S2b).

For each period and site, we estimated the 95% confidence intervals (CIs) of each AGB metric based on 1000 bootstraps over trees. CIs were made 20% broader to incorporate the 10% relative error based on the AGB_{TLS} estimates plus additional uncertainty related to observational error and process variability.

2.6 | Tree mortality and damage interactions

We tested how tightly tree damage is related to tree death. We first constructed generalized linear mixed-effects models (GLMMs) for each site to model the probability of death at the end of a given period as a function of the tree-level relative damage at the beginning of the period (i.e., damage-related AGB over initial AGB). We used a logit link function and species random intercepts and slopes following the same approach employed to define mortality risks in Zuleta, Arellano, et al. (2022). GLMMs were fitted by maximum likelihood estimation (Laplace approximation) using the LME4 package in R (Bates et al., 2022). In LME4 R notation, the formula was $m \approx 1 + relative\_damage + (1 + relative\_damage|s)$, where m is the probability of mortality and relative_damage is the damage condition of each individual tree of species s at the beginning of a period.

We finally assessed the proportion of total AGB losses from trees that get damaged but do not die after several years. We estimated AGB losses from all available combinations of consecutive censuses every two (15 periods, six sites), three (nine periods, five sites), and four (four periods, three sites) years within each site and compared the relative proportions of damage-related AGB loss and mortality-related AGB loss across these time census interval lengths.

3 | RESULTS

3.1 | Biomass loss from dead versus alive damaged trees

Total (dead + alive damaged) AGB loss rate averaged across periods and forests was 8.72 Mg ha^{-1} year^{-1} (95% CI 5.57–12.86), of which 58.5% was due to tree mortality (5.10 Mg ha^{-1} year^{-1}; 95% CI 2.84–8.31) and 41.5% was due to damage on living trees (3.62 Mg ha^{-1} year^{-1}; 95% CI 2.36–5.25) (Figure 1). Every year, an average of 3.8% of the individual trees died (SE = 0.3% year^{-1}; 2.5% trees SE = 0.2% year^{-1} for trees ≥10 cm dbh), whereas 8.1% (SE = 1.2% year^{-1}) of surviving trees lost at least 10% of their AGB in these forests (Figure S3).

3.2 | Spatial and temporal variability in AGB loss

AGB loss was highly variable among forests and over time, especially in Asia (Figures 2 and 3; Figure S3). Total AGB loss ranged from 4.54 Mg ha^{-1} year^{-1} (95% CI 2.77–6.90) in Huai Kha Khaeng (HKK, Thailand) to 12.81 Mg ha^{-1} year^{-1} (95% CI 7.72–19.53) in Khao Chong (KC, Thailand) (Figure 2) and from 1.91% year^{-1} (95% CI 1.17–2.90) in HKK to 5.78% year^{-1} (95% CI 4.09–7.77) in Fushan (Taiwan) when calculated as a percentage of initial biomass (Figure 3). Differences in total AGB loss among sites were mainly caused by site variability in damage-related AGB losses rather than by mortality-related AGB losses (Figure 3). Thus, the proportion of total AGB loss that resulted

from damage to living trees was also highly variable across sites. In five out of the seven forests studied (Amacayacu, BCI, and Yasuní in the Neotropics; and HKK and KC in Asia), damage-related AGB losses varied between 36% and 48%, and the 95% CIs of mortality-related and damage-related AGB losses overlapped in most of the periods within these sites (Figure 2). Extreme results were found in the two other sites in Asia, Fushan (Taiwan) and Pasoh (Malaysia), where damage-related AGB losses contributed to 76% and 12% of total AGB losses, respectively, a pattern that was consistent across periods within both sites (Figure 2).

3.3 | Tree damage and mortality interactions

The proportion of AGB lost to damage in a given tree significantly increased its probability of death in the next year across all sites (Figure 4a). The strong link between damage and mortality led to a decrease in the damage-related AGB loss as the time census interval length increased: from the 3.62 Mg ha^{-1} year^{-1} reported above at the 1-year census interval length to 2.16 Mg ha^{-1} year^{-1} (95% CI 1.48–3.00) and 1.93 Mg ha^{-1} year^{-1} (95% CI 1.36–2.61) at the 3-year and 4-year census interval lengths, respectively. However, mortality-related AGB loss also tended to decrease from 5.10 Mg ha^{-1} year^{-1} at the 1-year census interval length to 4.32 Mg ha^{-1} year^{-1} (95% CI 2.76–6.42) and 3.66 Mg ha^{-1} year^{-1} (95% CI 2.45–5.22) at the 3-year and 4-year census interval lengths, respectively. Therefore, the proportion of total AGB loss due to alive damaged trees maintained generally high (32% and 34%) when calculated at longer time census interval lengths (Figure 4b).

3.4 | Tree damage and estimates of AGB stocks and losses

On average, forest-level estimates of AGB stocks assuming undamaged trees (285.01 Mg ha^{-1}; 95% CI 220.58–353.45) were 4% higher
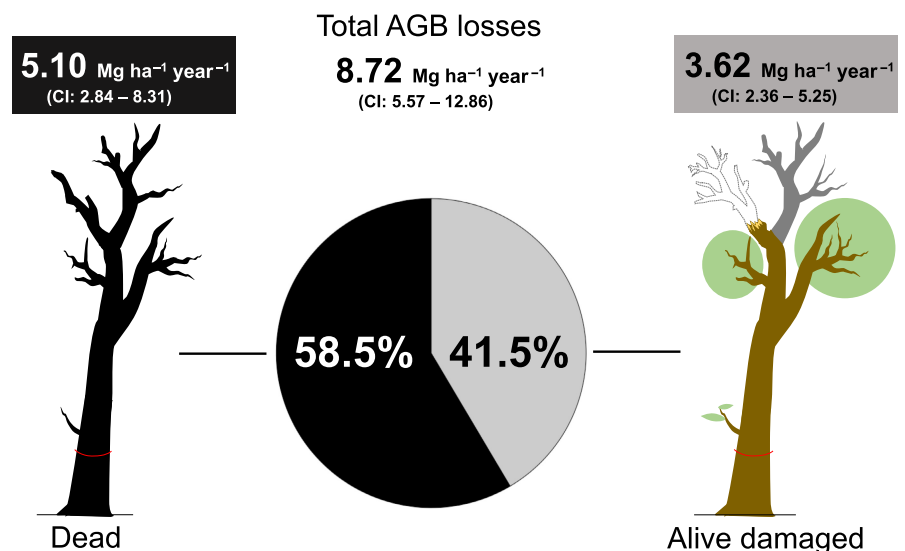

FIGURE 1 Aboveground biomass losses (Mg ha^{-1} year^{-1}) from dead (left, black) and alive damaged (right, gray) trees averaged across seven tropical forests. CI: 95% confidence intervals based on bootstrapping over trees in any given period and site. [Colour figure can be viewed at wileyonlinelibrary.com]
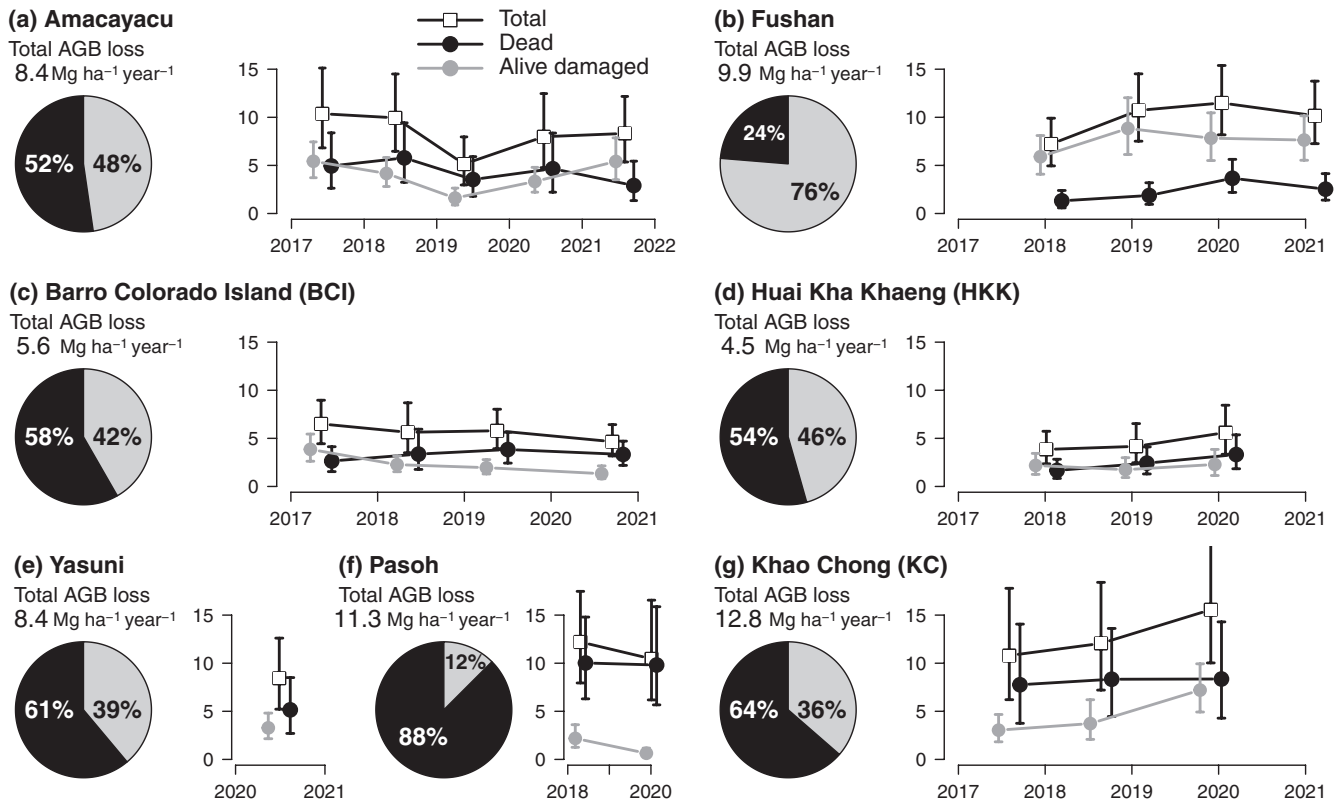
Total AGB losses
8.72 Mg ha^{-1} year^{-1}
(CI: 5.57 – 12.86)

5.10 Mg ha^{-1} year^{-1}
(CI: 2.84 – 8.31)

3.62 Mg ha^{-1} year^{-1}
(CI: 2.36 – 5.25)

58.5%   41.5%

Dead   Alive damaged

FIGURE 2 Temporal variability in aboveground biomass (AGB) losses across 22 one-year periods in seven tropical forest dynamics plots in the Neotropics (a,c,e) and Asia (b,d,f,g). For each site, panels show the total AGB loss rate (Mg ha^{-1} year^{-1}) averaged across periods, the proportion of total AGB lost from dead trees (black) and from damaged but living trees (gray) in the pie chart, and the AGB loss trends over time. For the temporal trends, points and squares show the average AGB loss rates (Mg ha^{-1} year^{-1}) centered in the mid-dates of each period; vertical bars show the 95% confidence limits based on bootstrapping over trees in each period. Sites are ordered alphabetically by name.
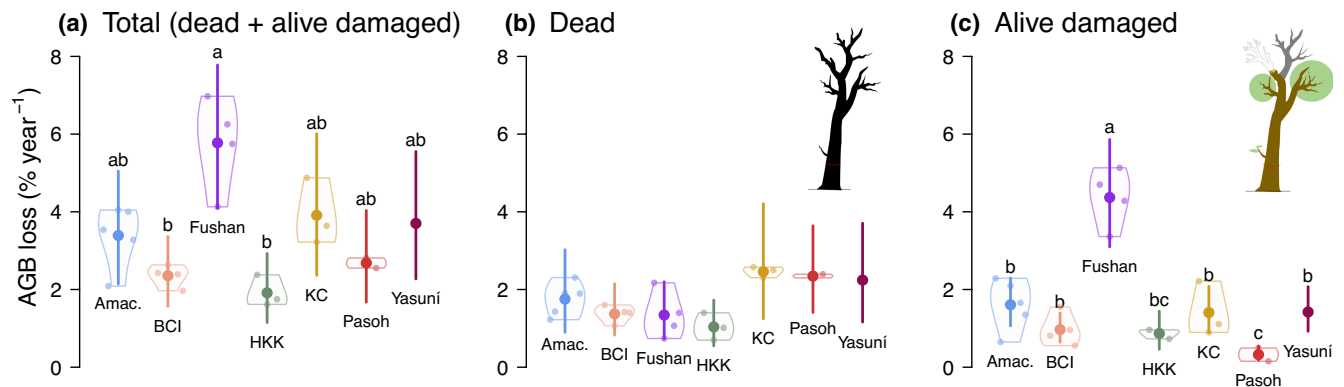

FIGURE 3 Total (a), mortality-related (b), and damage-related (c) aboveground biomass (AGB) loss rates (percentage of initial biomass) across 22 one-year periods in seven tropical forests. Solid points show the average AGB loss rate across periods within each site. Vertical bars show the averaged 95% confidence limits based on bootstrapping over trees in any given period and site. Violin plots show the distribution of AGB losses within each site, with transparent points showing the observed values in each period. Different letters indicate differences based on the 95% bootstrap confidence intervals across sites. Sites are ordered alphabetically by name. Amac.: Amacayacu; BCI: Barro Colorado Island; HKK: Huai Kha Khaeng; KC: Khao Chong. Note that Yasuní has only one period. [Colour figure can be viewed at wileyonlinelibrary.com]

than estimates accounting for tree damage (273.04 Mg ha^{-1}; 95% CI 211.51–338.58) (Figure 5a), with high variability across sites (1%–17%; Figure S4). In terms of AGB loss, conventional approaches

ignoring damage resulted in a 20%–29% underestimation of total AGB loss and a 16%–22% overestimation of mortality-related AGB loss depending on the time census interval length considered (Figure 5b,c).
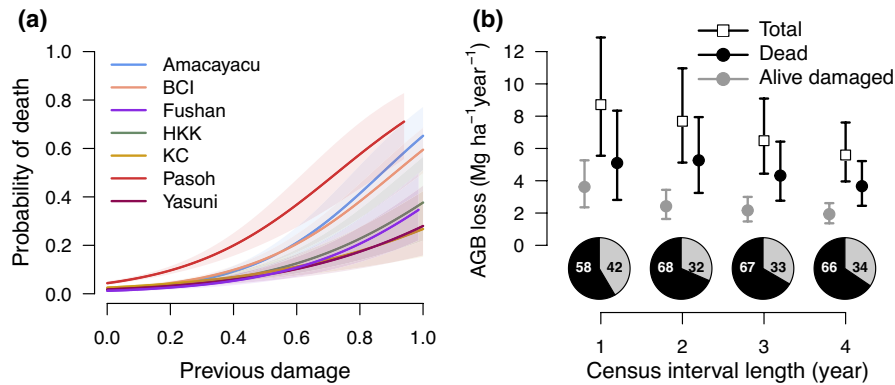
FIGURE 4 Tree damage and mortality interactions across seven tropical forests. (a) Site-level generalized linear mixed-effects models for the probability of death as a function of the relative aboveground biomass (AGB) lost in the previous year (i.e., previous damage). (b) AGB losses from all possible combinations of consecutive censuses at the 1-year (22 periods, seven sites), 2-year (15 periods, six sites), 3-year (nine periods, five sites), and 4-year (four periods, three sites) census interval lengths. For each census interval length, solid points and squares show the average AGB loss rates (Mg ha^{-1} year^{-1}); vertical bars show the 95% confidence limits based on bootstrapping over trees in each period. Pie charts show the percentage of total AGB losses from dead (left, black) and alive damaged (right, gray) trees averaged across periods for each census interval length. BCI: Barro Colorado Island; HKK: Huai Kha Khaeng; KC: Khao Chong. [Colour figure can be viewed at wileyonlinelibrary.com]
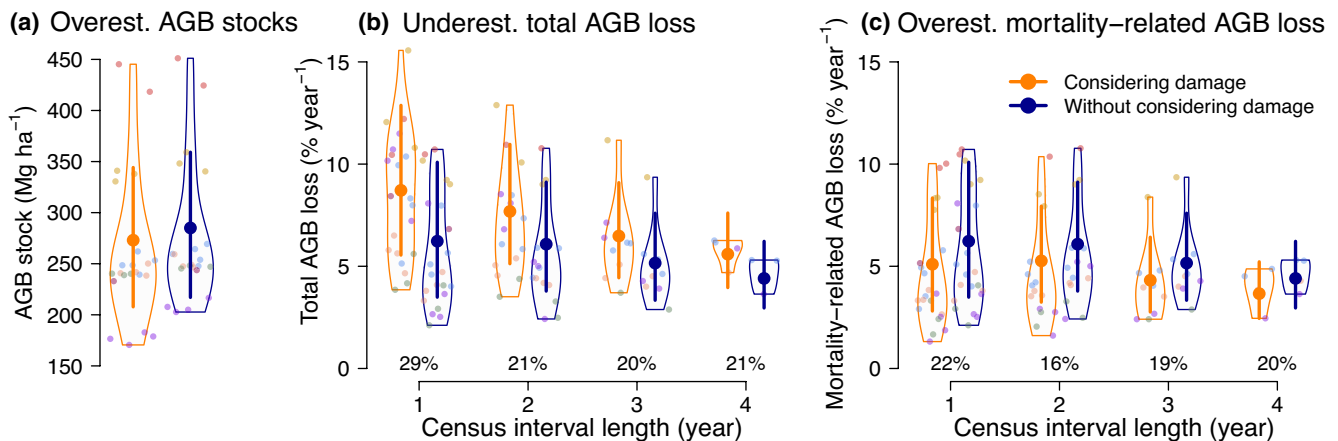

FIGURE 5 Aboveground biomass (AGB) stocks (a), total AGB loss rates (b), and mortality-related AGB loss rates (c) accounting for tree damage versus the conventional approach assuming undamaged trees. AGB loss rates are shown as a percentage of initial biomass. For each approach and census interval length, solid points show the average AGB loss rates, vertical bars show the 95% confidence limits (from bootstrapping over trees in each period), transparent points show the observed values in each period and site (site colors as in Figure 3), and violin plots show their distribution. In (b) and (c), numbers below each pair of violin plots show the average underestimation of total AGB loss rates in (b) and the average overestimation of mortality-related AGB loss rates in (c) for each census interval length. Note that conventional estimates of AGB loss (without considering damage) are the same in (b) and (c) because, under this approach, total AGB losses are assumed to be equivalent to the mortality-related AGB losses. [Colour figure can be viewed at wileyonlinelibrary.com]

4 | DISCUSSION

4.1 | The unaccounted forest biomass loss

Tree mortality is typically considered the only AGB loss in forest systems. By coupling field-based measurements of tree completeness with vertical volume profile models obtained from terrestrial laser scanning and biomass allometries for tropical trees, we show that 42% (range 12%–76% across forests) of total AGB loss is due to damage to living trees across seven tropical forests. Considering that the rate at which trees were damaged was higher than the rate at which

trees died, our main result indicates that, at the 1-year timescale, the amount of biomass lost from the few trees that died was almost equivalent to the amount of biomass lost from the many trees that got damaged but did not die.

Because highly damaged trees were more prone to die (Figure 4a; Arellano et al., 2019; Reis et al., 2022; Zuleta, Arellano, et al., 2022), damage-related AGB loss decreased when calculated at longer timescales. However, given that mortality-related AGB loss also decreased with increasing census interval lengths, the percentage of contribution of damage-related AGB losses relative to mortality-related AGB losses did not exhibit a decreasing trend

and was generally maintained between 32% and 34%. These results indicate that substantial proportions of trees that lost AGB in these forests survived and presumably recovered after 3–4 years; a resilience trait can be achieved via damage compartmentalization and/or resprouting (Paciorek et al., 2000; Shigo, 1984). Given that our damage estimates include dead branches that remain attached to the trees (Arellano et al., 2021), some of the AGB losses from surviving trees may be also associated with cladoptosis or "self-pruning," the process by which trees shed branches as they grow or in response to stressors such as droughts (Rood et al., 2000), liana infestation (Newbery & Zahnd, 2021), or diseases (Sprugel et al., 1991). The ecological consequences of AGB losses in living trees from external (winds, gaps, etc.) versus endogenous (physiological) factors as well as their interactions with species traits and life-history strategies deserve further investigation.

4.2 | Implications for estimates of forest biomass dynamics

Notably, our estimates of AGB loss from alive damaged trees (3.62 Mg ha^{-1} year^{-1}; 95% CI 2.36–5.25) more than triple the AGB change (ΔAGB) estimated across mature tropical rainforests in Asia (1.0 Mg ha^{-1} year^{-1} 95% CI 0.6–1.4), Africa (1.3 Mg ha^{-1} year^{-1} 95% CI 0.5–2.1), and the Neotropics (0.7 Mg ha^{-1} year^{-1} 95% CI 0.1–1.3) (Requena Suarez et al., 2019); and could potentially offset the net ecosystem carbon exchange in mature tropical broadleaf forests (Anderson-Teixeira et al., 2021). While branch production is generally expected to compensate branchfall in mature forests (Muller-Landau et al., 2021), our results revealed that the magnitude of this flux can be as important as that from tree mortality, suggesting a systematic overestimation of carbon residence times in forest ecosystems (Carvalhais et al., 2014; Yang et al., 2021). Resolving the magnitude and among-site variability of this flux as well as its ecological consequences (Needham et al., 2022) is critical to quantifying forest-based climate change mitigation potential.

Ignoring damage measurements yielded 4% (1%–17% range across forests) higher estimates of AGB stocks, 29% (6%–57% range across forests) lower estimates of total AGB losses, and 22% (7%–80% range across forests) higher estimates of mortality-related AGB losses compared to estimates considering damage. Our expectation is that heavily damaged trees are not included in the construction of AGB allometric models (Clark & Kellner, 2012). The degree to which they are included impacts how much excluding tree damage overestimates AGB stocks and underestimates AGB fluxes. Large discrepancies in AGB losses, the timing of damage-related and mortality-related AGB losses, and the high variability across forests, show the importance of better quantifying structural damage on living trees. Visible aboveground damage, together with other overlooked carbon fluxes at the tree level such as root damage and stem rot (Heineman et al., 2015), causes part of the mismatch between ground-based and remote sensing

estimates of forest carbon stocks and fluxes (Cabon et al., 2022) as well as the global carbon budget imbalance (Friedlingstein et al., 2022).

4.3 | Likely factors driving variability in AGB loss

Total AGB loss was highly variable among forests, but these differences were mainly caused by site variability in damage-related AGB losses rather than by mortality-related AGB losses. Differences across sites were most likely due to differences in disturbance regimes and species responses to environmental drivers (Feeley & Zuleta, 2022). Fushan, the site with the highest contribution of alive damaged trees to total AGB losses, has been impacted by nine typhoons and 18 tropical storms in the last 20 years (i.e., the center of the storm passed within a 50 km radius of the plot), with two of them occurring during the course of this study (*Nesat* typhoon in 2017-07-29 and *Lupit* tropical storm in 2021-08-07; Taiwan Center Weather Bureau). The prevalence of windstorms in this site results in disproportionate losses of AGB via damage that does not necessarily translate into individual tree mortality because many species in this site are adapted to withstand strong winds (e.g., multi-stemmed, short-stature, and sprouting; Su et al., 2020; Yap et al., 2016). High damage and low mortality have been documented for trees in other typhoon-disturbed forests (Hall et al., 2020; Hogan et al., 2018; Tanner et al., 2014; Yap et al., 2016). On the contrary, the high contribution of mortality-related AGB losses compared to damage-related AGB losses in Pasoh was due to a high tree mortality rate (5.82% year^{-1}, 95% CI 4.65–7.24 averaged over periods; Figure S3) during the census periods. This included the death of three of the biggest trees (diameter > 100 cm) in the plot that died without signs of prior damage. Whether specific disturbances (e.g., fire, droughts, insect outbreaks; Barrere et al., 2023) and/or sustained changes in climatic factors (e.g., atmospheric water stress; Bauman et al., 2022) are driving these patterns remains unclear, but we found no relationship between damage-related and mortality-related AGB loss rates among periods (even when excluding Fushan and Pasoh) (Figure S5; *p* > .10 in linear mixed-effect models controlling for temporal autocorrelation within sites) suggesting that these two sources of AGB loss may either result from different drivers or operate at different timescales (i.e., lagged effects). As data collection continues, comprehensive analyses of the underlying drivers of tree mortality and damage will be possible.

5 | CONCLUSION

Ground-based biomass stocks and fluxes are widely used to estimate carbon budgets, to quantify forest carbon offsets, and to calibrate and validate remote sensing products used to obtain biomass estimates at regional and global scales (Cabon et al., 2022; Chave et al., 2019; Duncanson et al., 2019; Labrière et al., 2022; Xu et al., 2021). In this study, we showed that biomass loss from damage to living trees

constitutes an important and overlooked component of biomass loss across seven tropical forests. Our results contrast with the typically low forest biomass losses estimated only from tree mortality and suggest that forest carbon turnover may be higher than previously thought. Since forest disturbance rates are expected to increase under changing climate (Seidl, 2017), the biomass loss to damage is likely to become more important. Accounting for biomass losses that are not necessarily captured by tree mortality is essential to improve estimates of carbon budgets as well as vegetation models aiming to predict the fate of forests under changing climate conditions.

AUTHOR CONTRIBUTIONS

Daniel Zuleta, Gabriel Arellano, and Stuart J. Davies conceptualized the study, performed formal analysis, and contributed to methodology, validation, and visualization. Daniel Zuleta, Gabriel Arellano, Salomón Aguilar, Sarayudh Bunyavejchewin, Nicolas Castaño, Chia-Hao Chang-Yang, Alvaro Duque, David Mitre, Musalmah Nasardin, Rolando Pérez, I-Fang Sun, Tze Leong Yao, Renato Valencia, Sruthi M. Krishna Moorthy, Hans Verbeeck, and Stuart J. Davies performed data curation and investigation. Stuart J. Davies, Salomón Aguilar, Nicolas Castaño, Chia-Hao Chang-Yang, Alvaro Duque, I-Fang Sun, Hans Verbeeck, and Renato Valencia contributed to funding acquisition and provided resources. Daniel Zuleta, Sruthi M. Krishna Moorthy, and Gabriel Arellano contributed to software. Daniel Zuleta wrote the original draft. All authors wrote, reviewed, and edited the manuscript.

CONFLICT OF INTEREST STATEMENT

The authors declare no competing interest.

DATA AVAILABILITY STATEMENT

TLS-derived tree point clouds and the corresponding QSMs are available in Zenodo at https://zenodo.org/record/6981485 (Krishna Moorthy et al., 2022). Data for the annual mortality and damage censuses are available in the NGEE Tropics Data Collection at https://doi.org/10.15486/ngt/1961178 (Zuleta et al., 2023). Main data for sites in the ForestGEO plot network are available through the online portal at: http://www.forestgeo.si.edu.

ORCID

Daniel Zuleta https://orcid.org/0000-0001-9832-6188
Gabriel Arellano https://orcid.org/0000-0003-3990-5344
Sean M. McMahon https://orcid.org/0000-0001-8302-6908
Sarayudh Bunyavejchewin https://orcid.org/0000-0002-1976-5041
Chia-Hao Chang-Yang https://orcid.org/0000-0003-3635-4946
Alvaro Duque https://orcid.org/0000-0001-5464-2058
I-Fang Sun https://orcid.org/0000-0001-9749-8324
Renato Valencia https://orcid.org/0000-0001-9770-6568
Sruthi M. Krishna Moorthy https://orcid.org/0000-0002-6838-2880
Hans Verbeeck https://orcid.org/0000-0003-1490-0168
Stuart J. Davies https://orcid.org/0000-0002-8596-7522

REFERENCES

Anderegg, W. R. L., Berry, J. A., Smith, D. D., Sperry, J. S., Anderegg, L. D. L., & Field, C. B. (2012). The roles of hydraulic and carbon stress in a widespread climate-induced forest die-off. *Proceedings of the National Academy of Sciences of the United States of America*, *109*, 233–237.

Anderson-Teixeira, K. J., Herrmann, V., Banbury Morgan, R., Bond-Lamberty, B., Cook-Patton, S. C., Ferson, A. E., Muller-Landau, H. C., & Wang, M. M. H. (2021). Carbon cycling in mature and re-growth forests globally. *Environmental Research Letters*, *16*, 053009.

Araujo, R. F., Grubinger, S., Celes, C. H. S., Negrón-Juárez, R. I., Garcia, M., Dandois, J. P., & Muller-Landau, H. C. (2021). Strong temporal variation in treefall and branchfall rates in a tropical forest is related to extreme rainfall: Results from 5 years of monthly drone data for a 50 ha plot. *Biogeosciences*, *18*, 6517–6531.

Arellano, G., Medina, N. G., Tan, S., Mohamad, M., & Davies, S. J. (2019). Crown damage and the mortality of tropical trees. *New Phytologist*, *221*, 169–179.

Arellano, G., Zuleta, D., & Davies, S. J. (2021). Tree death and damage: A standardized protocol for frequent surveys in tropical forests. *Journal of Vegetation Science*, *32*, e12981.

Barrere, J., Reineking, B., Cordonnier, T., Kulha, N., Honkaniemi, J., Peltoniemi, M., Korhonen, K. T., Ruiz-Benito, P., Zavala, M. A., & Kunstler, G. (2023). Functional traits and climate drive interspecific differences in disturbance-induced tree mortality. *Global Change Biology*, 1–16. https://doi.org/10.1111/gcb.16630

Bates, D., Maechler, M., Bolker, B., Walker, S., Christensen, R. H. B., Singmann, H., Dai, B., Scheipl, F., Grothendieck, G., Green, P., Fox, J., & Bauer, A. (2022). *lme4: Linear Mixed-Effects Models using "Eigen" and S4*.

Bauman, D., Fortunel, C., Delhaye, G., Malhi, Y., Cernusak, L. A., Bentley, L. P., Rifai, S. W., Aguirre-Gutiérrez, J., Menor, I. O., Phillips, O. L., McNellis, B. E., Bradford, M., Laurance, S. G. W., Hutchinson, M. F., Dempsey, R., Santos-Andrade, P. E., Ninantay-Rivera, H. R., Chambi Paucar, J. R., & McMahon, S. M. (2022). Tropical tree mortality has increased with rising atmospheric water stress. *Nature*, *608*, 528–533.

Cabon, A., Kannenberg, S. A., Arain, A., Babst, F., Baldocchi, D., Belmecheri, S., Delpierre, N., Guerrieri, R., Maxwell, J. T., McKenzie, S., Meinzer, F. C., Moore, D. J. P., Pappas, C., Rocha, A. V., Szejner, P., Ueyama, M., Ulrich, D., Vincke, C., Voelker, S. L., ... Anderegg, W. R. L. (2022). Cross-biome synthesis of source versus sink limits to tree growth. *Science*, *376*, 758–761.

Carvalhais, N., Forkel, M., Khomik, M., Bellarby, J., Jung, M., Migliavacca, M., Mu, M., Saatchi, S., Santoro, M., Thurner, M., Weber, U., Ahrens, B., Beer, C., Cescatti, A., Randerson, J. T., & Reichstein, M. (2014). Global covariation of carbon turnover times with climate in terrestrial ecosystems. *Nature*, *514*, 213–217.

Chambers, J. Q., dos Santos, J., Ribeiro, R. J., & Higuchi, N. (2001). Tree damage, allometric relationships, and above-ground net

primary production in Central Amazon forest. *Forest Ecology and Management*, 152, 73–84.

Chao, K.-J., Liao, P.-S., Chen, Y.-S., Song, G.-Z. M., Phillips, O. L., & Lin, H.-J. (2022). Very low stocks and inputs of necromass in wind-affected tropical forests. *Ecosystems*, 25, 488–503.

Chave, J., Condit, R., Lao, S., Caspersen, J. P., Foster, R. B., & Hubbell, S. P. (2003). Spatial and temporal variation of biomass in a tropical forest: Results from a large census plot in Panama. *Journal of Ecology*, 91, 240–252.

Chave, J., Davies, S. J., Phillips, O. L., Lewis, S. L., Sist, P., Schepaschenko, D., Armston, J., Baker, T. R., Coomes, D., Disney, M., Duncanson, L., Hérault, B., Labrière, N., Meyer, V., Réjou-Méchain, M., Scipal, K., & Saatchi, S. (2019). Ground data are essential for biomass remote sensing missions. *Surveys in Geophysics*, 40, 863–880.

Chave, J., Réjou-Méchain, M., Búrquez, A., Chidumayo, E., Colgan, M. S., Delitti, W. B. C., Duque, A., Eid, T., Fearnside, P. M., Goodman, R. C., Henry, M., Martínez-Yrízar, A., Mugasha, W. A., Muller-Landau, H. C., Mencuccini, M., Nelson, B. W., Ngomanda, A., Nogueira, E. M., Ortiz-Malavassi, E., … Vieilledent, G. (2014). Improved allometric models to estimate the aboveground biomass of tropical trees. *Global Change Biology*, 20, 3177–3190.

Clark, D. A., Brown, S., Kicklighter, D. W., Chambers, J. Q., Thomlinson, J. R., & Ni, J. (2001). Measuring net primary production in forests: Concepts and field methods. *Ecological Applications*, 11, 356–370.

Clark, D. A., Brown, S., Kicklighter, D. W., Chambers, J. Q., Thomlinson, J. R., Ni, J., & Holland, E. A. (2001). Net primary production in tropical forests: An evaluation and synthesis of existing field data. *Ecological Applications*, 11, 14–384.

Clark, D. B., & Kellner, J. R. (2012). Tropical forest biomass estimation and the fallacy of misplaced concreteness. *Journal of Vegetation Science*, 23, 1191–1196.

CloudCompare. (2021). *CloudCompare (version 2.10.2)*. [GPL software].

Csilléry, K., Kunstler, G., Courbaud, B., Allard, D., Lassègues, P., Haslinger, K., & Gardiner, B. (2017). Coupled effects of wind-storms and drought on tree mortality across 115 forest stands from the Western Alps and the Jura mountains. *Global Change Biology*, 23, 5092–5107.

Cushman, K. C., Bunyavejchewin, S., Cárdenas, D., Condit, R., Davies, S. J., Duque, Á., Hubbell, S. P., Kiratiprayoon, S., Lum, S. K. Y., & Muller-Landau, H. C. (2021). Variation in trunk taper of buttressed trees within and among five lowland tropical forests. *Biotropica*, 53, 1442–1453.

Cushman, K. C., Detto, M., García, M., & Muller-Landau, H. C. (2022). Soils and topography control natural disturbance rates and thereby forest structure in a lowland tropical landscape. *Ecology Letters*, 25, 1126–1138.

Dalagnol, R., Wagner, F. H., Galvão, L. S., Streher, A. S., Phillips, O. L., Gloor, E., Pugh, T. A. M., Ometto, J. P. H. B., & Aragão, L. E. O. C. (2021). Large-scale variations in the dynamics of Amazon forest canopy gaps from airborne lidar data and opportunities for tree mortality estimates. *Scientific Reports*, 11, 1388.

Davies, S. J., Abiem, I., Abu Salim, K., Aguilar, S., Allen, D., Alonso, A., Anderson-Teixeira, K., Andrade, A., Arellano, G., Ashton, P. S., Baker, P. J., Baker, M. E., Baltzer, J. L., Basset, Y., Bissiengou, P., Bohlman, S., Bourg, N. A., Brockelman, W. Y., Bunyavejchewin, S., … Zuleta, D. (2021). ForestGEO: Understanding forest diversity and dynamics through a global observatory network. *Biological Conservation*, 253, 108907.

Duncanson, L., Armston, J., Disney, M., Avitabile, V., Barbier, N., Calders, K., Carter, S., Chave, J., Herold, M., Crowther, T. W., Falkowski, M., Kellner, J. R., Labrière, N., Lucas, R., MacBean, N., McRoberts, R. E., Meyer, V., Næsset, E., Nickeson, J. E., … Williams, M. (2019). The importance of consistent global forest aboveground biomass product validation. *Surveys in Geophysics*, 40, 979–999.

Duque, A., Peña, M. A., Cuesta, F., González-Caro, S., Kennedy, P., Phillips, O. L., Calderón-Loor, M., Blundo, C., Carilla, J., Cayola, L.,

Farfán-Ríos, W., Fuentes, A., Grau, R., Homeier, J., Loza-Rivera, M. I., Malhi, Y., Malizia, A., Malizia, L., Martínez-Villa, J. A., … Feeley, K. J. (2021). Mature Andean forests as globally important carbon sinks and future carbon refuges. *Nature Communications*, 12, 2138.

Dyer, L. A., Carson, W. P., & Leigh, E. G. (2012). Insect outbreaks in tropical forests: Patterns, mechanisms, and consequences. In P. Barbosa, D. K. Letourneau, & A. A. Agrawal (Eds.), *Insect outbreaks revisited* (pp. 219–245). John Wiley & Sons, Ltd.

Espírito-Santo, F. D. B., Gloor, M., Keller, M., Malhi, Y., Saatchi, S., Nelson, B., Junior, R. C. O., Pereira, C., Lloyd, J., Frolking, S., Palace, M., Shimabukuro, Y. E., Duarte, V., Mendoza, A. M., López-González, G., Baker, T. R., Feldpausch, T. R., Brienen, R. J. W., Asner, G. P., … Phillips, O. L. (2014). Size and frequency of natural forest disturbances and the Amazon forest carbon balance. *Nature Communications*, 5, 3434.

Feeley, K. J., & Zuleta, D. (2022). Changing forests under climate change. *Nature Plants*, 8, 984–985.

Friedlingstein, P., Jones, M. W., O'Sullivan, M., Andrew, R. M., Bakker, D. C. E., Hauck, J., le Quéré, C., Peters, G. P., Peters, W., Pongratz, J., Sitch, S., Canadell, J. G., Ciais, P., Jackson, R. B., Alin, S. R., Anthoni, P., Bates, N. R., Becker, M., Bellouin, N., … Zeng, J. (2022). Global carbon budget 2021. *Earth System Science Data*, 14, 1917–2005.

Gora, E. M., Kneale, R. C., Larjavaara, M., & Muller-Landau, H. C. (2019). Dead wood necromass in a moist tropical forest: Stocks, fluxes, and spatiotemporal variability. *Ecosystems*, 22, 1189–1205.

Hall, J., Muscarella, R., Quebbeman, A., Arellano, G., Thompson, J., Zimmerman, J. K., & Uriarte, M. (2020). Hurricane-induced rainfall is a stronger predictor of tropical forest damage in Puerto Rico than maximum wind speeds. *Scientific Reports*, 10, 4318.

Harris, N. L., Gibbs, D. A., Baccini, A., Birdsey, R. A., de Bruin, S., Farina, M., Fatoyinbo, L., Hansen, M. C., Herold, M., Houghton, R. A., Potapov, P. V., Suarez, D. R., Roman-Cuesta, R. M., Saatchi, S. S., Slay, C. M., Turubanova, S. A., & Tyukavina, A. (2021). Global maps of twenty-first century forest carbon fluxes. *Nature Climate Change*, 11, 234–240.

Heineman, K. D., Russo, S. E., Baillie, I. C., Mamit, J. D., Chai, P. P.-K., Chai, L., Hindley, E. W., Lau, B. T., Tan, S., & Ashton, P. S. (2015). Evaluation of stem rot in 339 Bornean tree species: Implications of size, taxonomy, and soil-related variation for aboveground biomass estimates. *Biogeosciences*, 12, 5735–5751.

Hogan, J., Zimmerman, J., Thompson, J., Uriarte, M., Swenson, N., Condit, R., Hubbell, S., Johnson, D., Sun, I., Chang-Yang, C. H., Su, S. H., Ong, P., Rodriguez, L., Monoy, C., Yap, S., & Davies, S. (2018). The frequency of cyclonic wind storms shapes tropical forest dynamism and functional trait dispersion. *Forests*, 9, 404.

Hubau, W., Lewis, S. L., Phillips, O. L., Affum-Baffoe, K., Beeckman, H., Cuní-Sanchez, A., Daniels, A. K., Ewango, C. E. N., Fauset, S., Mukinzi, J. M., Sheil, D., Sonké, B., Sullivan, M. J. P., Sunderland, T. C. H., Taedoumg, H., Thomas, S. C., White, L. J. T., Abernethy, K. A., Adu-Bredu, S., … Zemagho, L. (2020). Asynchronous carbon sink saturation in African and Amazonian tropical forests. *Nature*, 579, 80–87.

Kohyama, T. S., Kohyama, T. I., & Sheil, D. (2019). Estimating net biomass production and loss from repeated measurements of trees in forests and woodlands: Formulae, biases and recommendations. *Forest Ecology and Management*, 433, 729–740.

Kolby Smith, W., Reed, S. C., Cleveland, C. C., Ballantyne, A. P., Anderegg, W. R. L., Wieder, W. R., Liu, Y. Y., & Running, S. W. (2016). Large divergence of satellite and Earth system model estimates of global terrestrial CO_2 fertilization. *Nature Climate Change*, 6, 306–310.

Krishna Moorthy, S. M., Calders, K., Vicari, M. B., & Verbeeck, H. (2020). Improved supervised learning-based approach for leaf and wood classification from LiDAR point clouds of forests. *IEEE Transactions on Geoscience and Remote Sensing*, 58, 3057–3070.

Krishna Moorthy, S. M., Meunier, F., Calders, K., Aguilar, A., Pausenberger, N., Schnitzer, S. A., Visser, M. D., Muller-Landau, H. C., & Verbeeck, H. (2022). Datasets to quantify the impact of lianas on 3D tree structure and biomass. *Zenodo*. https://doi.org/10.5281/zenodo.6981485

Labrière, N., Davies, S. J., Disney, M. I., Duncanson, L. I., Herold, M., Lewis, S. L., Phillips, O. L., Quegan, S., Saatchi, S. S., Schepaschenko, D. G., Scipal, K., Sist, P., & Chave, J. (2022). Toward a forest biomass reference measurement system for remote sensing applications. *Global Change Biology*, *29*, 827–840.

Leitold, V., Morton, D. C., Martinuzzi, S., Paynter, I., Uriarte, M., Keller, M., Ferraz, A., Cook, B. D., Corp, L. A., & González, G. (2022). Tracking the rates and mechanisms of canopy damage and recovery following hurricane Maria using multitemporal Lidar data. *Ecosystems*, *25*, 892–910.

Maass, J. M., Martínez-Yrízar, A., Patiño, C., & Sarukhán, J. (2002). Distribution and annual net accumulation of above-ground dead phytomass and its influence on throughfall quality in a Mexican tropical deciduous forest ecosystem. *Journal of Tropical Ecology*, *18*, 821–834.

Malhi, Y., Farfán Amézquita, F., Doughty, C. E., Silva-Espejo, J. E., Girardin, C. A. J., Metcalfe, D. B., Aragão, L. E. O. C., Huaraca-Quispe, L. P., Alzamora-Taype, I., Eguiluz-Mora, L., Marthews, T. R., Halladay, K., Quesada, C. A., Robertson, A. L., Fisher, J. B., Zaragoza-Castells, J., Rojas-Villagra, C. M., Pelaez-Tapia, Y., Salinas, N., … Phillips, O. L. (2014). The productivity, metabolism and carbon cycle of two lowland tropical forest plots in south-western Amazonia, Peru. *Plant Ecology & Diversity*, *7*, 85–105.

Marvin, D. C., & Asner, G. P. (2016). Branchfall dominates annual carbon flux across lowland Amazonian forests. *Environmental Research Letters*, *11*, 094027.

McDowell, N., Pockman, W. T., Allen, C. D., Breshears, D. D., Cobb, N., Kolb, T., Plaut, J., Sperry, J., West, A., Williams, D. G., & Yepez, E. A. (2008). Mechanisms of plant survival and mortality during drought: Why do some plants survive while others succumb to drought? *New Phytologist*, *178*, 719–739.

McDowell, N. G., Sapes, G., Pivovaroff, A., Adams, H. D., Allen, C. D., Anderegg, W. R. L., Arend, M., Breshears, D. D., Brodribb, T., Choat, B., Cochard, H., de Cáceres, M., de Kauwe, M. G., Grossiord, C., Hammond, W. M., Hartmann, H., Hoch, G., Kahmen, A., Klein, T., … Xu, C. (2022). Mechanisms of woody-plant mortality under rising drought, CO_2 and vapour pressure deficit. *Nature Reviews Earth & Environment*, *3*, 294–308.

McEwan, R. W., Lin, Y.-C., Sun, I.-F., Hsieh, C.-F., Su, S.-H., Chang, L.-W., Song, G. Z. M., Wang, H. H., Hwong, J. L., Lin, K. C., Yang, K. C., & Chiang, J. M. (2011). Topographic and biotic regulation of aboveground carbon storage in subtropical broad-leaved forests of Taiwan. *Forest Ecology and Management*, *262*, 1817–1825.

Muller-Landau, H. C., Cushman, K. C., Arroyo, E. E., Martinez Cano, I., Anderson-Teixeira, K. J., & Backiel, B. (2021). Patterns and mechanisms of spatial variation in tropical forest productivity, woody residence time, and biomass. *New Phytologist*, *229*, 3065–3087.

Needham, J. F., Arellano, G., Davies, S. J., Fisher, R. A., Hammer, V., Knox, R. G., Mitre, D., Muller-Landau, H. C., Zuleta, D., & Koven, C. D. (2022). Tree crown damage and its effects on forest carbon cycling in a tropical forest. *Global Change Biology*, *28*, 5560–5574.

Newbery, D. M., & Zahnd, C. (2021). Change in liana density over 30 years in a Bornean rain forest supports the escape hypothesis. *Ecosphere*, *12*, e03537.

Paciorek, C. J., Condit, R., Hubbell, S. P., & Foster, R. B. (2000). The demographics of resprouting in tree and shrub species of a moist tropical forest. *Journal of Ecology*, *88*, 765–777.

Palace, M., Keller, M., & Silva, H. (2008). Necromass production: Studies in undisturbed and logged Amazon forests. *Ecological Applications*, *18*, 873–884.

Piponiot, C., Anderson-Teixeira, K. J., Davies, S. J., Allen, D., Bourg, N. A., Burslem, D. F. R. P., Cárdenas, D., Chang-Yang, C. H., Chuyong, G., Cordell, S., Dattaraja, H. S., Duque, Á., Ediriweera, S., Ewango, C., Ezedin, Z., Filip, J., Giardina, C. P., Howe, R., Hsieh, C. F., … Muller-Landau, H. C. (2022). Distribution of biomass dynamics in relation to tree size in forests across the world. *New Phytologist*, *234*, 1664–1677.

Raumonen, P., Kaasalainen, M., Åkerblom, M., Kaasalainen, S., Kaartinen, H., Vastaranta, M., Holopainen, M., Disney, M., & Lewis, P. (2013). Fast automatic precision tree models from terrestrial laser scanner data. *Remote Sensing*, *5*, 491–520.

Reis, S. M., Marimon, B. S., Esquivel-Muelbert, A., Marimon, B. H., Jr., Morandi, P. S., Elias, F., de Oliveira, E. A., Galbraith, D., Feldpausch, T. R., Menor, I. O., Malhi, Y., & Phillips, O. L. (2022). Climate and crown damage drive tree mortality in southern Amazonian edge forests. *Journal of Ecology*, *110*, 876–888.

Réjou-Méchain, M., Tanguy, A., Piponiot, C., Chave, J., & Hérault, B. (2017). biomass: An r package for estimating above-ground biomass and its uncertainty in tropical forests. *Methods in Ecology and Evolution*, *8*, 1163–1167.

Requena Suarez, D., Rozendaal, D. M. A., De Sy, V., Phillips, O. L., Alvarez-Dávila, E., Anderson-Teixeira, K., Arroyo, L., Baker, T. R., Bongers, F., Brienen, R. J. W., Carter, S., Cook-Patton, S. C., Feldpausch, T. R., Griscom, B. W., Harris, N., Hérault, B., Honorio Coronado, E. N., Leavitt, S. M., Lewis, S. L., … Herold, M. (2019). Estimating aboveground net biomass change for tropical and subtropical forests: Refinement of IPCC default rates using forest plot data. *Global Change Biology*, *25*, 3609–3624.

Rood, S. B., Patiño, S., Coombs, K., & Tyree, M. T. (2000). Branch sacrifice: Cavitation-associated drought adaptation of riparian cottonwoods. *Trees*, *14*, 248–257.

Seidl, R. (2017). Forest disturbances under climate change. *Nature Climate Change*, *7*, 395–402.

Shigo, A. L. (1984). Compartmentalization: A conceptual framework for understanding how trees grow and defend themselves. *Annual Review of Phytopathology*, *22*, 189–214.

Solé, R. V., & Manrubia, S. C. (1995). Are rainforests self-organized in a critical state? *Journal of Theoretical Biology*, *173*, 31–40.

Sprugel, D. G., Hinckley, T. M., & Schaap, W. (1991). The theory and practice of branch autonomy. *Annual Review of Ecology and Systematics*, *22*, 309–334.

Su, S., Guan, B. T., Chang-Yang, C., Sun, I., Wang, H., & Hsieh, C. (2020). Multi-stemming and size enhance survival of dominant tree species in a frequently typhoon-disturbed forest. *Journal of Vegetation Science*, *31*, 429–439.

Tanner, E. V. J., Rodriguez-Sanchez, F., Healey, J. R., Holdaway, R. J., & Bellingham, P. J. (2014). Long-term hurricane damage effects on tropical forest tree growth and mortality. *Ecology*, *95*, 2974–2983.

Ver Planck, N. R., & MacFarlane, D. W. (2014). Modelling vertical allocation of tree stem and branch volume for hardwoods. *Forestry*, *87*, 459–469.

Xu, L., Saatchi, S. S., Yang, Y., Yu, Y., Pongratz, J., Bloom, A. A., Bowman, K., Worden, J., Liu, J., Yin, Y., Domke, G., McRoberts, R. E., Woodall, C., Nabuurs, G. J., de-Miguel, S., Keller, M., Harris, N., Maxwell, S., & Schimel, D. (2021). Changes in global terrestrial live biomass over the 21st century. *Science Advances*, *7*, eabe9829.

Yang, H., Ciais, P., Wang, Y., Huang, Y., Wigneron, J., Bastos, A., Chave, J., Chang, J., Doughty, C. E., Fan, L., Goll, D., Joetzjer, E., Li, W., Lucas, R., Quegan, S., Le Toan, T., & Yu, K. (2021). Variations of carbon allocation and turnover time across tropical forests. *Global Ecology and Biogeography*, *30*, 1271–1285.

Yap, S. L., Davies, S. J., & Condit, R. (2016). Dynamic response of a Philippine dipterocarp forest to typhoon disturbance. *Journal of Vegetation Science*, *27*, 133–143.

Zanne, A. E., Lopez-Gonzalez, G., Coomes, D. A., Ilic, H., Jansen, S., Lewis, S., Miller, R., Swenson, N., Wiemann, M., & Chave, J. (2009). Global wood density database. *Dryad* [Data set].

Zuleta, D., Arellano, G., Aguilar, S., Bunyavejchewin, S., Castaño, N., Chang-Yang, C.-H., Duque, A., Mitre, D., Nasardin, M., Pérez, R., Sun, I.-F., Yao, T. L., Valencia, R., McMahon, S. M., & Davies, S. J. (2023). *Tree damage and mortality measurements across seven ForestGEO plots in the tropics between Oct 2016 and Mar 2023*.

Zuleta, D., Arellano, G., Muller-Landau, H. C., McMahon, S. M., Aguilar, S., Bunyavejchewin, S., Cárdenas, D., Chang-Yang, C. H., Duque, A., Mitre, D., Nasardin, M., Pérez, R., Sun, I. F., Yao, T. L., & Davies, S. J.

(2022). Individual tree damage dominates mortality risk factors across six tropical forests. *New Phytologist*, *233*, 705–721.

Zuleta, D., Krishna Moorthy, S. M., Arellano, G., Verbeeck, H., & Davies, S. J. (2022). Vertical distribution of trunk and crown volume in tropical trees. *Forest Ecology and Management*, *508*, 120056.

SUPPORTING INFORMATION

Additional supporting information can be found online in the Supporting Information section at the end of this article.